# New evidence of CO2 soil degassing anomalies on Piton de la Fournaise volcano and the link with volcano tectonic structures

Marco Liuzzo, Andrea Di Muro, G Giudice, Laurent Michon, Valérie Ferrazzini, S Gurrieri

AGU PUBLICATIONS

Geochemistry, Geophysics, Geosystems

RESEARCH ARTICLE

10.1002/2015GC006032

**Key Points:**
- $CO_2$ soil degassing anomalies at Piton de la Fournaise
- $\delta^{13}C$ magmatic signature
- Close link between anomalous $CO_2$ degassing and the main seismotectonic structures

**Supporting Information:**
- Supporting Information S1
- Figure S1
- Table S1
- Table S2
- Table S3
- Table S4

**Correspondence to:**
M. Liuzzo,
marco.liuzzo@ingv.it

**Citation:**
Liuzzo, M., A. Di Muro, G. Giudice, L. Michon, V. Ferrazzini, and S. Gurrieri (2015), New evidence of $CO_2$ soil degassing anomalies on Piton de la Fournaise volcano and the link with volcano tectonic structures, *Geochem. Geophys. Geosyst.*, *16*, 4388–4404, doi:10.1002/2015GC006032.

Received 28 JUL 2015
Accepted 24 NOV 2015
Accepted article online 8 DEC 2015
Published online 31 DEC 2015



# New evidence of $CO_2$ soil degassing anomalies on Piton de la Fournaise volcano and the link with volcano tectonic structures

**M. Liuzzo[1], A. Di Muro[2], G. Giudice[1], L. Michon[3], V. Ferrazzini[2], and S. Gurrieri[1]**

[1]Istituto Nazionale de Geofisica e Vulcanologia - Sezione di Palermo, Italy, [2]Institut de Physique du Globe de Paris, Observatoire Volcanologique du Piton de la Fournaise, Sorbonne Paris-Cité, CNRS UMR-7154, Université Paris Diderot, Paris, France, [3]Laboratoire Géosciences Réunion, Université de La Réunion, Institut de Physique du Globe de Paris, Sorbonne Paris Cité, CNRS, F-97744 Saint-Denis, France

**Abstract** Piton de la Fournaise (PdF) is recognized as one of the world's most active volcanoes in terms of eruptive frequency and the substantial quantity of lava produced. Yet with the sole exception of rather modest intracrateric fumarole activity, this seems to be in contrast with an apparent absence of any type of natural fluid emission during periods of quiescence. Measurement campaigns were undertaken during a long-lasting quiescent period (2012–2014) and just after a short-lived summit eruption (June 2014) in order to identify potential degassing areas in relation to the main structural features of the volcano (e.g., rift zones) with the aim of developing a broader understanding of the geometry of the plumbing and degassing system. In order to assess the possible existence of anomalous soil $CO_2$ flux, 513 measurements were taken along transects roughly orthogonal to the known tectonic lineaments crossing PdF edifice. In addition, 53 samples of gas for C isotope analysis were taken at measurement points that showed a relatively high $CO_2$ concentration in the soil. $CO_2$ flux values range from 10 to 1300 g $m^{-2}$ $d^{-1}$ while $\delta^{13}C$ are between $-26.6$ and $-8‰$. The results of our investigation clearly indicate that there is a strong spatial correlation between the anomalous high values of diffusive soil emissions and the main rift zones cutting the PdF massif and, moreover, that generally high soil $CO_2$ fluxes show a $\delta^{13}C$ signature clearly related to a magmatic origin.

## 1. Introduction

Piton de la Fournaise (PdF) volcano is recognized as one of the most active volcanoes in the world, with one eruption every 9 months on average [*Peltier et al.*, 2010; *Roult et al.*, 2012]. It is also well known as a volcano that has very weak peripheral volcanic fluid emissions and with only modest gas release in intracrateric fumaroles during the quiescent periods between eruptive activity [*Barillon et al.*, 1993; *Di Muro et al.*, 2012; *Liuzzo et al.*, 2014; *Marty et al.*, 1993; *Seidel et al.*, 1988; *Toutain et al.*, 2002]. By contrast, Piton des Neiges volcano, the dormant twin of PdF, presents many springs and sites with volcanic fluid emissions, whose geochemical signature clearly record deep inputs of magmatic fluids [*Marty et al.*, 1993; *Toutain et al.*, 2002].

Given the limited presence of fluid emissions at PdF, it is understandable that only few studies have focused their attention on the search for gaseous emissions, particularly in the peripheral areas of the volcano. Thus, PdF is a very insufficiently studied volcano in terms of geochemical investigation of soil $CO_2$ flux. This is notably in contrast with increased interest in research on other active volcanoes of the world recognizing the important relationship between diffuse soil degassing and active tectonic areas [*Allard et al.*, 1991; *Chiodini et al.*, 2004] and the potential this offers for volcano monitoring [*Gurrieri et al.*, 2008; *Liuzzo et al.*, 2013; *Viveiros et al.*, 2008, 2014].

A previous study, which focused on in situ soil gas measurements for $CO_2$, $^{4}He$, and $^{222}Rn$ [*Toutain et al.*, 2002], concluded that diffuse degassing is of likely organic origin at PdF but also suggested that a further review should be conducted, taking into account the possible isotopic signature of C in $CO_2$ not investigated by the authors. In addition, *Toutain et al.* [2002] investigated the NE and SE rift zones but did not perform measurements on the NW-SE rift zone, which is the largest and the one with the deepest seismicity [*Michon et al.*, 2015]. In this work, we focus on identifying the possible presence of $CO_2$ emitted from soils, particularly in relation to the main rift zones that cross the flanks of the volcano edifice (NE, SE, and NW-SE) and converge toward the summit area. A main target of our research was to identify a possible contribution of volcanic gas distinguishable from the organic component and contextualize these within a framework that considers the geological and seismotectonic features of the area. The work consisted of a series of surveys that covered the flanks of the volcano and the summit area of PdF during which more than 500 measurements were taken over three campaigns. These were carried out between 2012 and 2014 in the same season (end of August to beginning of September, dry season) in order to obtain samples emitted during similar environmental conditions and to minimize the potential effect of intense tropical rain events. In addition, 53 gas samples were taken for isotopic analysis of $\delta^{13}C$ in $CO_2$. The results of the investigation reveal a spatial pattern of anomalous $CO_2$ degassing consistent with the main tectonic structures intersecting PdF, which also corresponds to areas with the highest concentration of pyroclastic cones. Furthermore, there is a particularly interesting correspondence was found between the highest levels of anomalous $CO_2$ degassing and the distribution of eccentric earthquakes occurring at depths greater than 15 km. Finally, the isotopic analysis results of $\delta^{13}C$ in $CO_2$ from the soil, the first in our knowledge for PdF, show a recognizable deep volcanic component, which suggests that there is a potential connection between the areas of anomalous degassing on the volcano flank and the deep plumbing system of this volcano.

## 2. Geological Context

La Réunion Island is the emerged part of a large intraplate volcanic complex located in the southwestern part of the Indian Ocean. It is geologically situated in the Mascarene Basin and attributed to the activity of the same hot spot which generated the Deccan Traps [*Courtillot et al*., 1986; *Duncan et al*., 1989; *Lénat et al*., 2001]. In this geodynamic context, Mauritius and La Réunion islands represent the youngest expression of volcanism in the Mascarene Basin. Three volcanoes have been identified in the formation of La Réunion edifice; these are Les Alizés, Piton des Neiges, and Piton de la Fournaise. Les Alizés, which is only recognized by gravity, magnetic, and drillhole investigations, is an old buried volcano forming part of the south-eastern submarine flank of the edifice [*Gailler et al*., 2009; *Gailler and Lénat*, 2010; *Lénat et al*., 2001; *Malengreau et al*., 1999; *Rançon et al*., 1989]. This old edifice is considered to be about the same age as the largest volcano of the island, Piton des Neiges (~2 Ma), which reaches an altitude of 3069 m above sea level (a.s.l), on the western side of the island. Recent dating of the last eruptions, relatively frequent seismic activity and the occurrence of $CO_2$-rich thermal sources suggest that Piton des Neiges is currently in a quiescent phase [*Marty et al*., 1993]. The youngest volcano of La Réunion is the very active basaltic shield, Piton de la Fournaise (PdF), which forms the SE part of the island and has a maximum height of 2632 m. Geochemical signatures in ultramafic xenoliths [*Hanyu et al*., 2001; *Hopp and Trieloff*, 2005; *Trieloff et al*., 2002] and erupted magmas [*Albarède et al*., 1997; *Bosch et al*., 2008; *Di Muro et al*., 2014; *Pietruszka et al*., 2009; *Vlastélic et al*., 2009] indicate that the volcanic activity of La Réunion is related to a relatively homogeneous mantle source which has changed only little over time.

The island of La Réunion is strongly influenced by its volcanic nature and by the extreme precipitation rates, which result in a rugged topography of cliffs and deep canyons. The climate of La Réunion is both tropical and oceanic, with an average annual temperature of about 30°C and is subject to steep temperature gradients in relation to altitude. Annual precipitation along the windward eastern coast can reach 11 m/yr (MeteoFrance). These extreme climatic conditions facilitate substratum degradation and soil formation on most surfaces, despite the fact that the terrain is relatively young.

La Réunion Island has the largest area of intact vegetation among the islands in the Mascarene archipelago despite substantial deforestation that affected most parts of the island following human settlement in the sixteenth century. Much of the island has been subsequently reforested and now contains almost 40% forest cover [*Baret et al*., 2006]. The vegetation itself varies considerably from coastal wetlands and swamp forest, through lowland rain forest and palm savannah to deciduous montane forest and heathland vegetation types at the highest elevations [*Strasberg et al*., 2005]. On the PdF massif, soils are predominantly andosols in various stages of development while cambisol, umbrisol, and phaeozem are more common at low altitude (<900 m a.s.l). Total carbon content is usually lower than 5.3% in most soils and decreases with increasing depth [*Doelsch et al*., 2006]. The largest proportion of organic matter in the volcanic soil can be sequestrated by minerals in organomineral complexes [*Basile-Doelsch et al*., 2007]. *Basile-Doelsch et al*. [2007] have shown that in the andosol of La Réunion, poorly crystalline aluminosilicate minerals have a strong binding potential to organic matter because of their large specific surface area and great reactivity.

## 3. Measurement Methods

Measurements of soil $CO_2$ flux were carried out using the "dynamic concentration" method [*Gurrieri and Valenza*, 1988] based on an empirically identified relationship between soil $CO_2$ flux and $CO_2$ concentration in a gas mixture obtained by diluting soil gas with air (dynamic concentration) by means of a specific 50 cm long probe inserted into the soil. Through a constant flux rate of 0.8 L/min, the gas from the soil is pumped to an IR spectrophotometer that measures the concentration of $CO_2$. The spectrophotometer used was manufactured by Edinburgh Instruments Ltd. (range 0–10%; accuracy ±2%; digital resolution 0.01%) and pressure and temperature corrected. The $CO_2$ flux is hence derived from the $CO_2$ dynamic concentration value through an empirical relationship (1) verified experimentally in the laboratory for a range of applicable permeability 0.36–123 $\mu m^2$ and pumping flux 0.4–4.0 L/min:

$$\phi CO_2 = (32–5.8\ k^{0.24})\ C_d + 6.3\ k^{0.6} C_d^3 \quad (1)$$

where $\phi CO_2$ is the soil $CO_2$ flux expressed in kg $m^{-2}$ $d^{-1}$, *k* is the numerical values of the gas permeability ($\mu m^2$), and $C_d$ is the numerical value of molar fraction of the diluted $CO_2$ concentration. We used a value of k = 35, which corresponds to the average of gas permeability values that were determined experimentally in Italy [*Camarda et al*., 2006a, 2006b; M. Camarda, personal communication, 2015] and in Japan [*Moldrup et al*., 2003]. In this work, $\phi CO_2$ is converted into g $m^{-2}$ $d^{-1}$ (for more details on the method, see *Camarda et al*. [2006a, 2006b]).

Gas samples for isotopic analysis were taken by introducing a Teflon capillary probe into the ground (50 cm long to $\phi$1.0 mm) and collected in 10 mL vials to be analyzed at INGV Palermo laboratories. Carbon isotope composition of $CO_2$ (and $CO_2$ concentration) was determined by using a Thermo Delta Plus XP CF-IRMS (precision ± 0.15 δ‰) coupled with a Thermo TRACE Gas Chromatograph (GC) and a Thermo GC/C III interface, as described in *Ilyinskaya et al*. [2015].

Transects were chosen in order to intersect the directions identified by maximum concentration of cinder cones on the volcano flanks (rift zones) [*Michon et al*., 2015]. Where possible, measurements were performed with a spacing of ca. 100 m; the maximum length of a single transect was 8.9 km.

## 4. Results From the Field Work

### 4.1. Soil $CO_2$ Flux

Throughout three different field trips, which were spaced annually between 2012 and 2014, a total of 513 soil $CO_2$ flux measurements were taken (Figure 1). Distances between individual sites and length and orientation of the tracks were dependent upon local urban density, morphological obstacles, and vegetation cover. Soil thickness and vegetation cover tend to decrease when moving from low to high elevation. Meters thick red soils with agricultural or natural (tropical) dense vegetation cover occur near sea level while the central area close to the volcano summit is almost desertic with very little vegetation and variable thicknesses of lapillis and soils (usually <1 m thick) on lava flow substratum. At most of the measurement sites we recorded some meteorological parameters (temperature, pressure, humidity, and wind speed) in order to evaluate any possible interference with the in situ $CO_2$ flux. In addition, samples of gas for isotopic analysis were collected at points where $CO_2$ flux was approximately higher than 80.0 g $m^{-2}$ $d^{-1}$ (supporting information Table S1). The measurements on the Piton des Neiges area (Piton Saint Leu and L'Etang Salé red rectangle in Figure 1) were taken to test the intensity and distribution of anomalous soil $CO_2$ flux near narrow volcanic lineaments on the quiescent volcano.

Several studies have demonstrated that diffusive volcanic gas transfer on active volcanoes preferentially occurs in proximity to tectonic structures [*Bonforte et al*., 2013; *Giammanco et al*., 1998; *Irwin and Barnes*, 1980], therefore generating relative levels of anomalous flux with respect to biogenic background. Thus, the distribution of measurements along transects roughly perpendicular to the main tectonic alignments generally shows some measurements with values significantly higher in proximity to the faults, where those of lower magnitude represent the background level. In our survey, we performed several transects crossing the main tectonic structures of PdF, which are considered the main direction of the deep magma propagation in dykes [*Michon et al*., 2007; *Bonali et al*., 2011; *Michon et al*., 2015]. Two examples of results from the measurement transects performed on PdF (blue square in Figure 1) are plotted in Figure 2. As the cases

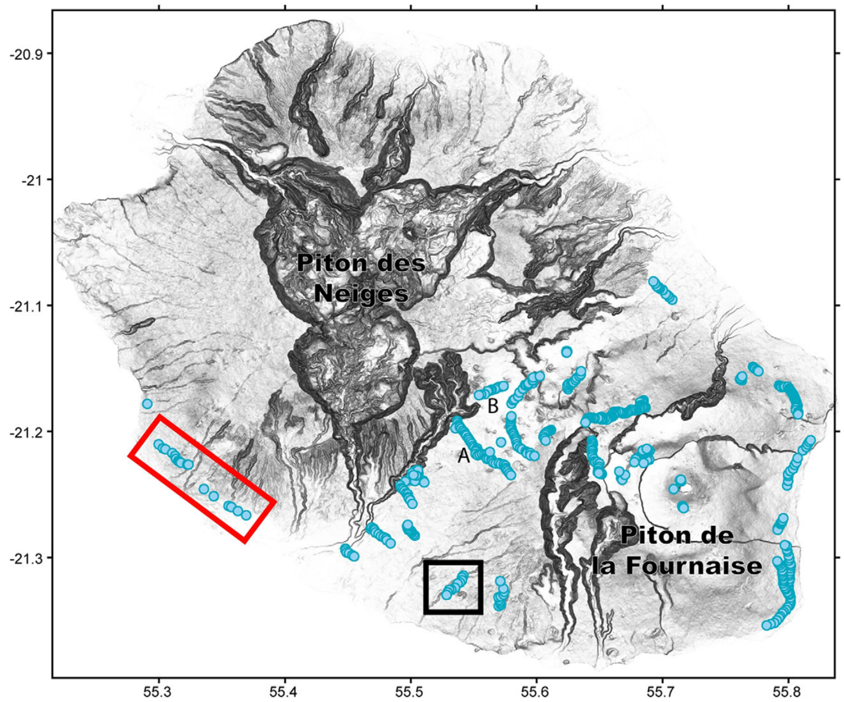


**Figure 1.** La Réunion Island: map showing the location of soil gas measurements. The letters A and B indicate the site of the measurements used for the transects on PdF massif reported in Figure 2. Red rectangle: Piton Saint Leu and L'Etang Salé, the sites for preliminary tests on the main cone alignments cutting the quiescent volcano, Piton de Neiges. Black rectangle indicates the position of Mont Vert area discussed in the text.

mentioned before, transects at PdF show measurements that might be considered as anomalous (points above the grey area), being significantly higher compared to the neighboring measurements, which can be considered as a background level. However, in order to quantify which measurements should be considered anomalous, we proceeded following two steps:

1. We assessed the potential influence of environmental parameters which may affect the value of $CO_2$ flux (pressure, temperature, wind speed).
2. We performed a statistical analysis of our database in order to identify the threshold value for anomalous flux with respect to background $CO_2$ flux.

We found no correlation (Figure 2) between the $CO_2$ flux and the main meteorological parameters, which changed relatively little during our field campaigns. The coefficient of variation (CV) is lower than 0.2% regarding pressure and lower than 12% regarding temperature and humidity, while wind speed reaches CV values of up to 63%, and is the only parameter that showed a fair variability. However, all these meteorological parameters have a coefficient of determination ($R^2$) with the $CO_2$ flux that is lower than 0.2. During the relatively short duration of profile measurements (a few hours), it is reasonable to conclude that meteorological parameters did not affect $CO_2$ flux spatial change. Moreover, it is important to remember that the IR spectrophotometer used is pressure and temperature corrected, therefore allowing us to consider the whole measurements normalized to the same pressure and temperature condition.

Having established that any meteorological influence on $CO_2$ flux is negligible, we can then define a threshold for the all measurements of the surveys in order to identify any anomalous values. To this end, we adopted a generally accepted statistical method using a Normal Probability plot (NPP—Figure 3, inset) for the analysis of the measurement distributions. The graph obtained does not show any linear trend, which signifies that our data set shows a departure from normality. It is conventionally accepted to consider the flex point of the curve a reasonable point of change between different populations of (under certain assumptions) different degassing regimes. In order to distinguish between different populations of flux rates, a first approximation of a possible threshold in our data set can be identified at $CO_2$ flux of ca. 78 g $m^{-2}$ $d^{-1}$. However, in order to discriminate between different classes of $CO_2$ flux, we also performed a

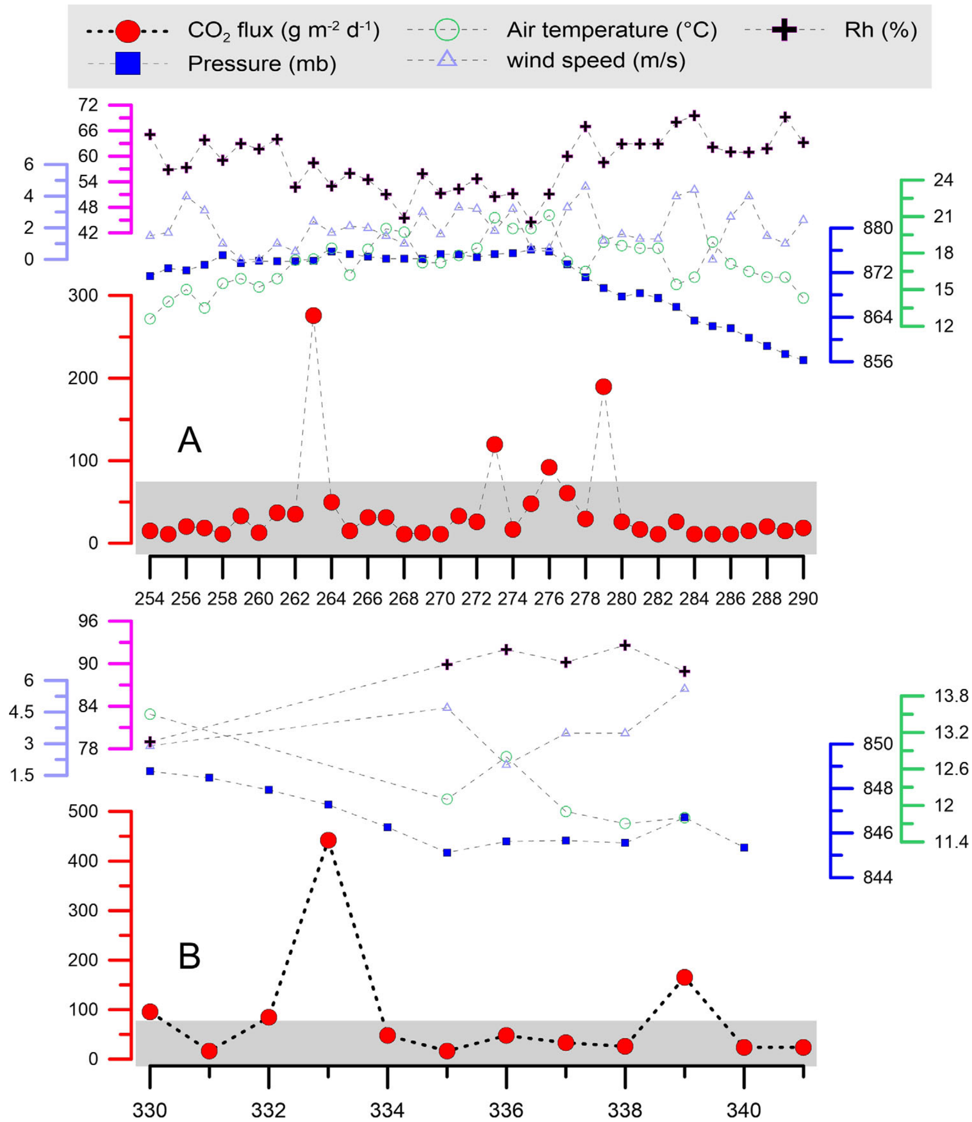


**Figure 2.** Plot of two transects of soil $CO_2$ flux measurements (letters A and B in Figure 1) performed on PdF massif. The two examples show that some measurements are significantly higher in relation to the more common measurements at lower $CO_2$ flux, which can be considered as the background level for the area (grey area). The graphs also show that the little changing meteorological parameters have no effect on the measurements. Grey box represents the unit measurements for each parameter; *X* axis indicates the sequential number of measurements.

procedure suggested in *Sinclair* [1974] (see supporting information Table S3 and Figure S1). We then further used the different populations found with the Sinclair procedure in order to produce a map that identifies different ranges of data. For the purpose of this graphical representation, we choose to unite the lower $CO_2$ flux populations identified (F5 and F6 in supporting information Figure S1) in a single class with $CO_2$ flux up to 55 g $m^{-2}$ $d^{-1}$. Figure 3 shows a map obtained with the above described procedure, which provides a simple and immediate way to compare the distribution of the anomalous $CO_2$ flux with other parameters such as seismicity and volcanic activity. On the volcano massif, many sites showed relatively high values of $CO_2$ flux. Moreover, the threshold chosen here is significantly higher than the typical values of about 20–30 g $m^{-2}$ $d^{-1}$, which several authors on other sites worldwide [*Mielnick and Dugas*, 2000; *Rey et al.*, 2002] have previously attributed to normal biological activity. However, the low values proposed by these authors cannot be used as a reliable threshold in tropical volcanic environments, and does not allow a reliable distinction between biogenic and volcanic sources in our area.

The spatial distribution of the highest anomalies in the map displays significant concentrations (i) on the northwestern flank of PdF at high elevation and (ii) on the northeast border of PdF, along the coast. It is

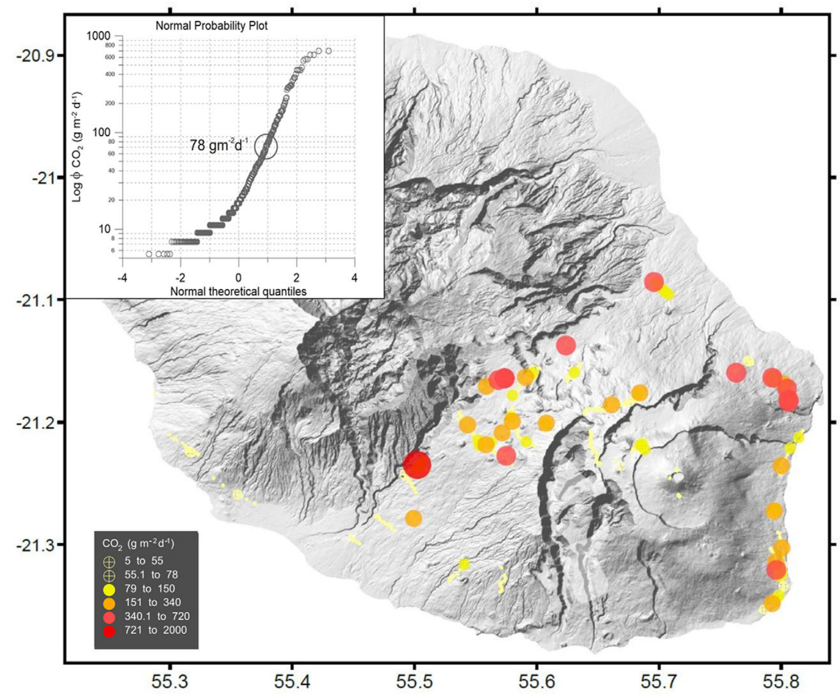


**Figure 3.** Map of soil $CO_2$ measurements. The figure shows a classed postmap where the $CO_2$ fluxes are distinguished in different ranges of degassing rates. The inset shows a Normal Probability Plot used to find a statistical threshold in order to discriminate between anomalous and nonanomalous fluxes. The different ranges of degassing rates have been identified using the procedure proposed by *Sinclair* [1974], the results of this analysis are provided as supporting information (supporting information Figure S1 and Table S3).

interesting to note that the $CO_2$ flux values decrease when approaching the Central Cone of Piton de la Fournaise in the Enclos Fouqué caldera, where the $CO_2$ flux attains very low values. This is consistent with the period of inactivity of PdF since a last intrusion event in January 2011 [*Roult et al*., 2012].

### 4.2. Isotopic Data

The attempt to seek evidence of a magmatic origin for soil $CO_2$ flux in a location where existing geochemical literature had thus far been unable to affirm its occurrence, led to the decision to focus on high $CO_2$ flux samples in order maximize the probability of detecting traces of magmatic component. Therefore, we collected samples from 53 sites for isotopic analyses (supporting information Table S2) where $\phi CO_2$ was greater than 80 g $m^{-2}$ $d^{-1}$. In total, we performed 106 isotopic analyses, taking two samples for each of the 53 sites in order to verify the sampling consistency. All the samples were taken directly from the soil, as described in section 3, with the exception of three taken inside a tunnel belonging to the public electric company of France (EDF; Rivière de l'Est tunnel), where we observed a water gurgling phenomenon. In this case, the gases were sampled using a funnel. The results of their C-concentration and isotopic analyses are shown in Figure 4, where data are reported as delta (δ) permil (‰) values. Our entire data set shows $\delta^{13}C$ values spanning between 26.6 and 8‰ for a range of $CO_2$ concentrations comprising between 1209 and 109,480 ppm. In the graph, our analysis is compared with $\delta^{13}C$ value from summit fumaroles inside the Dolomieu crater of PdF, which are the only data known from the literature [*Marty et al*., 1993]. In their work, the authors took three samples with contents of ~90% air and ~10% $CO_2$ and a $\delta^{13}C$ constant at 4.1‰ (triangles in Figure 4). The authors also stressed that the $\delta^{13}C$ signature of the PdF fumaroles is comparable to the isotopic signature from PdN summit springs. Unfortunately, access to and sampling of the fumarolic field has been impossible since the major summit caldera collapse in 2007. The few available data on hot fumaroles and springs suggest a spatial and temporal homogeneity of the isotopic features in both PdN and PdF, and in particular, that $\delta^{13}C$ value measured in Dolomieu samples can be considered as representative of the initial $\delta^{13}C$ for PdF magmas. Figure 4 displays the distribution of our $\delta^{13}C$ measurements, covering a wide range from typical biogenic sources to that of summit fumaroles. Our data suggest that the main process controlling isotopic variability is the mixing between these two end-members, more than the

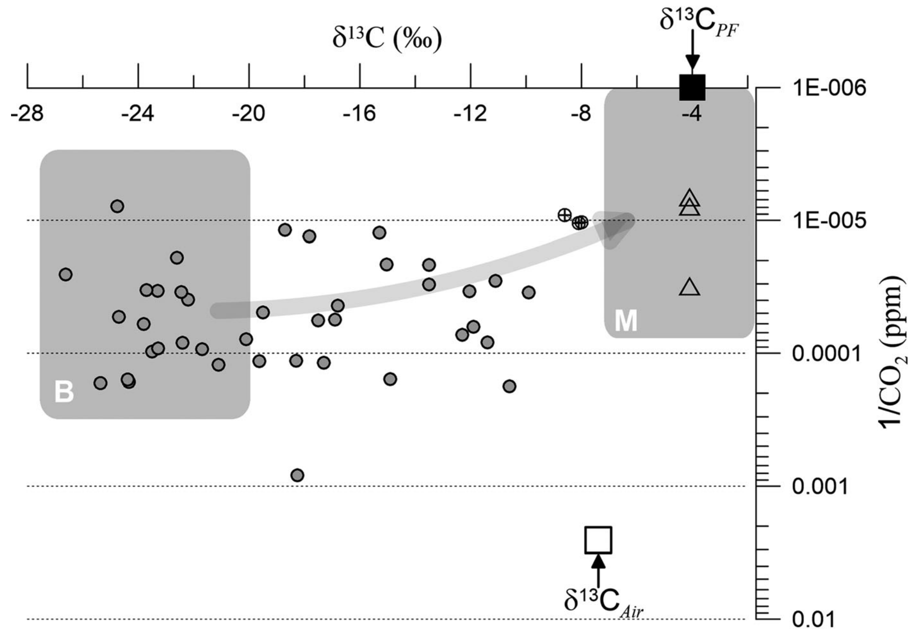


**Figure 4.** Diagram plotting the carbon isotopic composition of soil $CO_2$ versus $1/CO_2$ soil concentrations (ppm). All the grey filled circles are the samples of $CO_2$ taken from the soil, while the crossed circles are the samples collected inside a tunnel belonging to the public electric company of France (EDF). The empty square is a sample of air collected close the volcanological observatory of PdF used as atmospheric reference of $CO_2$. The full black square is the $\delta^{13}C$ of the PdF fumarole from *Marty et al*. [1993] restored at 100% of $CO_2$ concentration. The triangles are the isotopic compositions of the samples at the real $CO_2$ concentrations not yet corrected for the air contents (see *Marty et al*. [1993] for major specifications). B and M included in the grey squares indicate the probable end-members-areas of, respectively, biogenic and magmatic sources.

mixing with air. In order to better constrain the mixing lines between these three possible sources (magmatic, organic, and air), we can consider isotopic values ($\delta^{13}C_{cs}$) measured on charcoal samples taken from PdF ashes younger than 7 kyr [*Morandi et al*., 2016]. We use $\delta^{13}C_{PF}$ (black square in Figure 4, which consists of the restored data at 100% of $CO_2$) [*Marty et al*., 1993] and $\delta^{13}C_{cs}$ as an approximation of two possible isotopic signature end-members (volcanic and biogenic, respectively). In this way, we can calculate two theoretical curves of binary mixing between atmospheric and volcanic end-members (thick grey curves in Figure 5) and between atmospheric and biogenic end-members, where for the latter we considered the average of $\delta^{13}C_{cs}$ values (thick dotted curves in Figure 5). The isotopic data carried out in our survey are almost systematically more positive than the air-biogenic binary mixing curve and shifted toward volcanic values (Figure 5). A main source of uncertainty is related to the variability of the isotopic signature of our biogenic end-members in consideration of several factors that can potentially affect the $\delta^{13}C$ of $CO_2$ diffused from the soil. In the case of PdF, and considering that the island is an intraplate basaltic volcano situated in a humid tropical context, we can infer that the main two factors that may determine a significant change on the isotopic signature of $CO_2$ are either (i) isotopic fractionation in presence of aquifers and or (ii) the effect of a thick vegetation cover able to influence the soil $CO_2$ flux [*Amundson et al*., 1998; *Cerling et al*., 1991; *Chiodini et al*., 2008]. Both processes will affect the isotopic signature of the soil $CO_2$ flux and will produce more negative values. For these reasons, further investigations are necessary to be able to discriminate between the different degrees of isotopic fractionation that potentially occur in the studied area. However, it is important to observe some aspects of our data set in relation to the environmental features of the island: (i) the gas samples were taken always in sites where the $CO_2$ flux was significantly high according to our statistical treatment, and, therefore, in principle, most likely to attributed to a volcanic origin; (ii) very thick agricultural (sugarcane) red soils sampled at low altitude in the Mont Vert area (southern flank of the massif, Figure 1 black square) did not show any abnormal $CO_2$ flux, suggesting no clear correlation between anomalous $CO_2$ flux measurements and the most vegetated area; (iii) the samples for the isotopic analysis were taken from the first meter of soil and therefore the role played by organic material must be taken into account. As demonstrated by many studies, poorly crystalline aluminosilicates in the soil are particularly efficient in trapping organic matter [*Basile-Doelsch et al*., 2005; *Frank et al*., 2002, 2006; *Rouff et al*.,

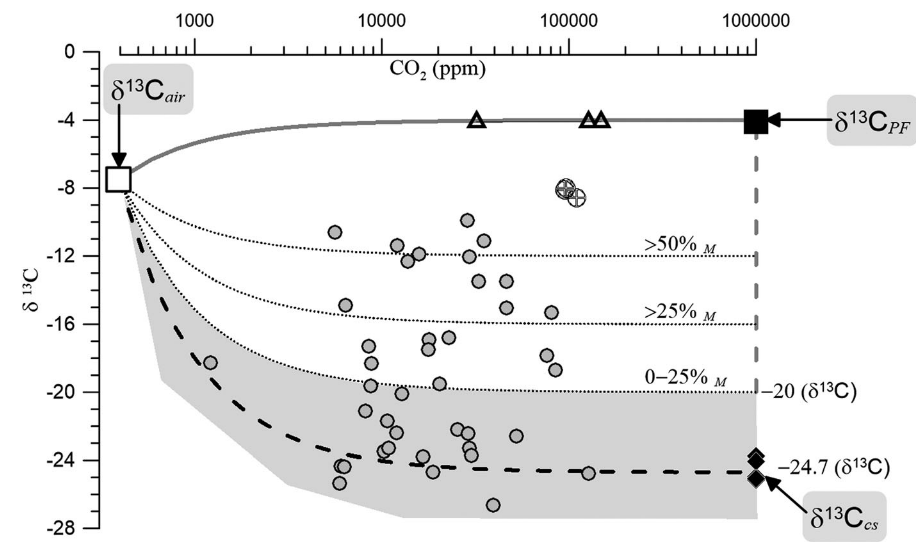


**Figure 5.** Diagram plotting carbon isotopic composition of soil $CO_2$ versus $CO_2$ soil log-concentrations (ppm) showing the theoretical binary mixing curves between atmospheric and biogenic (thick black dotted curves), atmospheric and magmatic (thick grey curves), and biogenic and magmatic end-members (thick grey dotted curves). Also shown are the binary mixing curves (hyphen curve) which allow a differentiation in the percentage of the magmatic component (M) in the hypothesis that the biogenic contribution could be extended up to $\delta^{13}C$ 20‰ (see text for discussion). The diamond symbols are charcoal samples of recent PdF eruptions [*Morandi et al.*, 2016]. The other symbols are the same as in Figure 4.

2012]. We can therefore reasonably expect that deep $CO_2$ volcanic gas will mix in the last part of its path toward the surface with $CO_2$ flux produced by organic matter (with a distinct isotopic signature). Therefore, the shallow part of the soil might strongly affects the carbon isotope composition measurements, particularly in a tropical environment like Piton de la Fournaise. In fact, *Basile-Doelsch et al.* [2005] found on PdN values of $\delta^{13}C$ between 27 to 25.2 in the first 52 cm of soils developed on old volcanic ashes.

A further indication of an organic component in relation to our measurements can be identified through a statistical analysis (Figure 6 and supporting information Table S4) using a probability plot showing the distribution of the carbon isotopic composition. Here we recognize four different populations of values using the procedure suggested in *Sinclair* [1974]. The first population, F1, relates to the more negative isotopic values ranging between approximately −26 and −22‰, and can be considered representative of the biogenic end-members.

Taking into consideration the previously outlined premises and our statistical results, we can reasonably conclude that a biogenic source is likely to be characterized by a range of isotopic signatures extending as far as −20‰ (hyphen curve; grey area Figure 5). It is then possible to argue that the samples above this limit have an isotopic signature that indicates a variable proportion of magmatic contribution. Figure 5 also shows two other mixing curves that quantify the percentage of the magmatic component under the hypothesis of atmospheric-biogenic-magmatic mixing, thereby indicating that a considerable number of sites on the PdF massif are characterized by a clearly recognizable magmatic component.

Even though these data cannot be considered conclusive, as indeed more data could give a stronger statistical constraint to the different populations of isotopic data, both the high $CO_2$ flux rate and the positive isotopic signature strongly suggest the presence of far from negligible amounts of volcanic gas emanations streaming through the flanks of PdF (up to ~50 wt %). Moreover, these fluxes can represent a significant indication of a connection between the degassing area and a deep magmatic source on the PdF massif, as already proposed by *Marty et al.* [1993] for Piton des Neiges and more recently by *Michon et al.* [2015] for Piton de la Fournaise.

## 5. Cross Correlation in an Interpretative Model and Discussion

Seismic and structural features of La Réunion Island show peculiarities that need to be considered in order to assess the geochemical data in an inclusive context. In order to place our data in relation to the broader

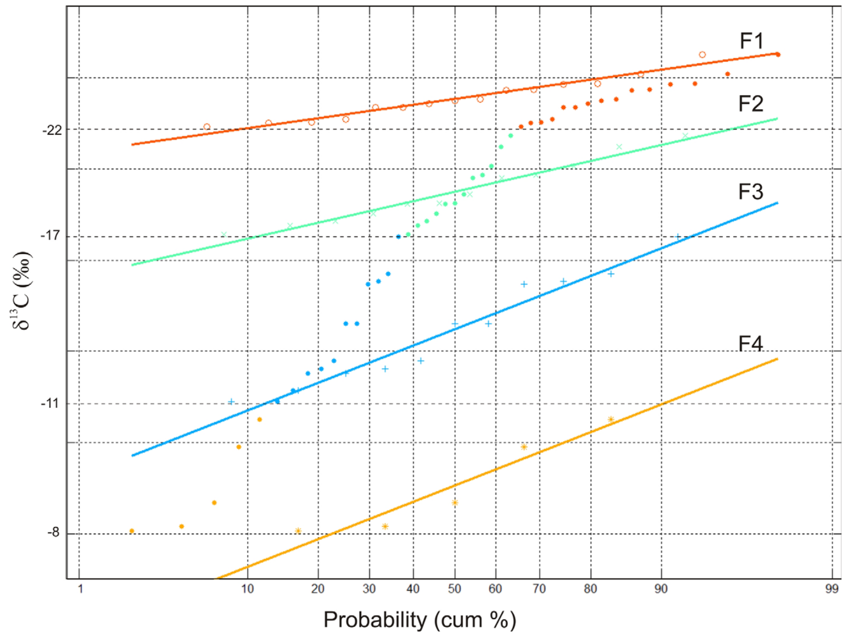


**Figure 6.** Probability plot of the carbon isotopic composition. In the diagram, four populations of values F1– F4 are reported. The F1 (in red) is well constrained and can be attributed to the biogenic source ($\delta^{13}C$ interval range between −26.6 and −22.2‰; see also supporting information Table S4). F2 and F3 could be interpreted as a mixture populations between the biogenic and the magmatic end-members, while the F4 ($\delta^{13}C$ interval range between −10.6 and −8‰) is the population of values with the highest magmatic contribution.

geological context of the volcano, we considered three different features of PdF: (i) the distribution of the volcano-tectonic events over the last 8 years; (ii) the spatial distribution of the volcanic cones, which is a proxy to identify the preferential intrusion paths; (iii) the main volcano-tectonic structures.

### 5.1. Earthquakes and $CO_2$ Flux

Being widely distributed over the whole island, the seismic monitoring network of Piton de la Fournaise Volcano Observatory allows seismic events to be located with a precision ranging from 200 m below the volcano summit [*Massin et al.*, 2011], where the seismic network is densest, to several kilometers over the remaining study area [*Michon et al.*, 2015]. For our purpose, we used the PdF Volcano Observatory seismic catalog of manually located events recorded between 2006 and 2014, when the duration magnitude was higher than 1. The lowest duration magnitude may be negative for shallow events under the summit crater where the density of seismic stations is high, and of the order of 1 for deeper events far from the Enclos Fouqué central caldera. In this work, we considered the same ranges of depths discussed by *Michon et al.* [2015] in order to disclose possible correlation between the earthquakes and the $CO_2$ flux distribution in the island. Figure 7 shows the maps obtained superimposing $CO_2$ flux and earthquakes. We stress that seismic activity was at very low levels during the 2012–2014 quiescent period (<4–8 shallow volcano tectonic events per day, located below the central cone). Swarms of deep VT events were recorded below the NW-SE rift only between March and April 2014, 2 months before the reactivation of the volcano. VT events related to the 1 day long June 2014 eruption (~3 months before our last field campaign) were very shallow and located at ~1.5 km below volcano summit.

The "shallow" seismic activity with hypocenters located between the surface and 11 km below sea level (bsl) is concentrated close to the PdF central cone (Figure 7a) and correlates with the occurrence of frequent summit or proximal eruptions [*Roult et al.*, 2012]. The absence in this area of any anomaly in terms of $CO_2$ flux is remarkable (Figure 3). Even if our data are consistent with previous results [*Toutain et al.*, 2002], it must be stressed that during our survey in the proximity of the volcano we were able to perform only a few measurements along the highly fractured rim of the PdF crater, where the high degree of mixing with air can affect our results. In any case, this upper part of the crater is known for being devoid of any degassing phenomenon [*Toutain et al.*, 2002] other than weak intracrateric fumaroles [*Di Muro et al.*, 2012; *Staudacher et al.*, 2009]. These findings suggest the possibility that the summit area of the crater is quite "open,"

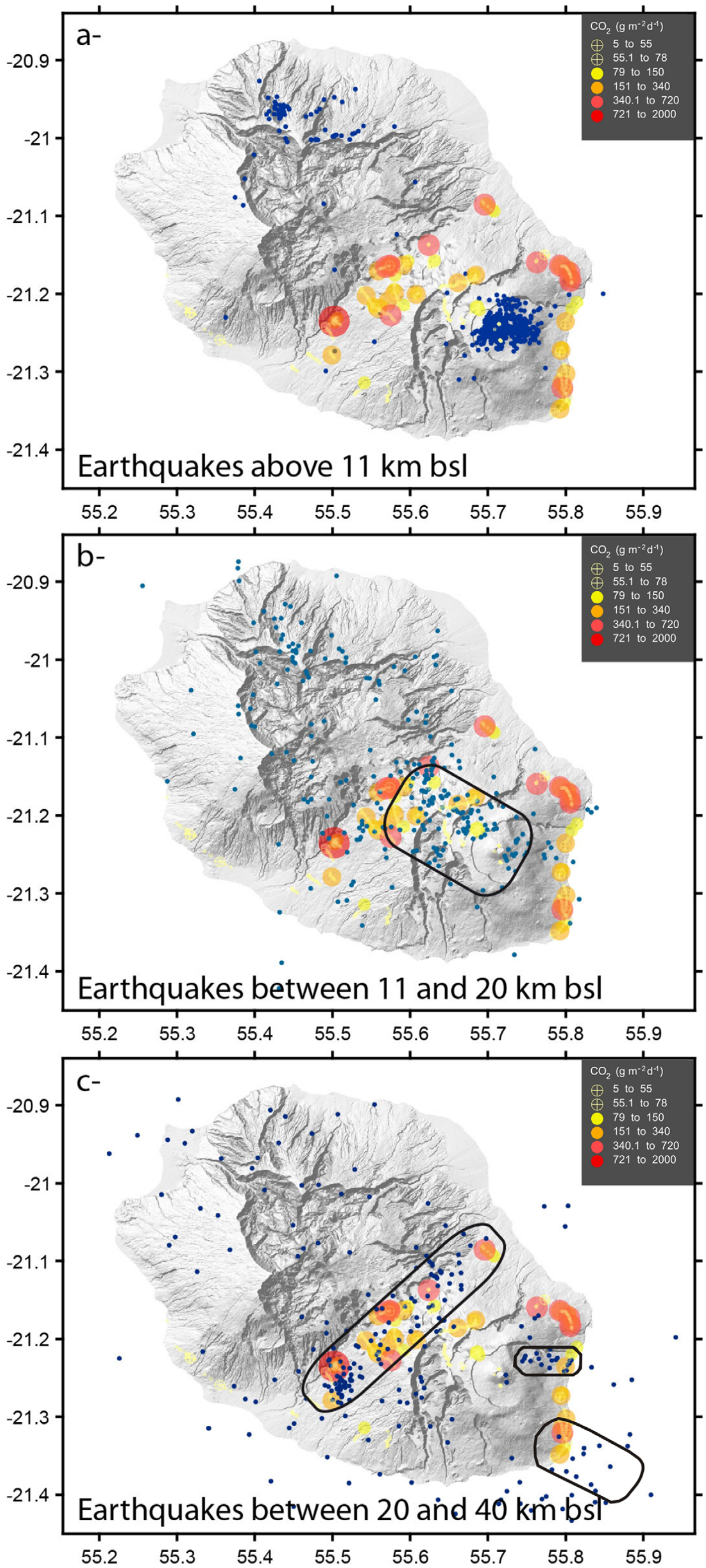


**Figure 7.** Map of $CO_2$ fluxes and hypocenter location of the earthquakes. Three different classes of earthquakes are selected in relation to the depth position of the hypocenters: (a) earthquakes above 11 km; (b) between 11 and 20 km; (c) between 20 and 40 km bsl. In Figures 7b and 7c, the area limited by the thick black line underlines the sectors of PdF where $CO_2$ flux and earthquakes show a quite good superimposition (see text for interpretation).

possibly because of the very frequent summit collapses (last collapse in 2007) [*Michon et al*., 2013] and of the highly fractured structure, which facilitates the dispersion of the deep degassing. Recently, *Savage et al*. [2015] interpreted the spatial distribution of low Vp/Vs seismic ratios at PdF as an evidence of deep pressurized gas-filled cracks poorly connected with the surface. On the other hand, the very low level of summit degassing mirrors the low level of volcanic activity after the major 2007 eruption [*Roult et al*., 2012].

Between 11 and 20 km bsl (Figure 7b), in the mantle lithosphere, hypocenters appear scattered over the entire PdF volcano, even if some clusters can be clearly identified along a NW-SE trending zone running from PdN to PdF summits (Plaine des Cafres). This area is characterized by moderate $CO_2$ flux anomalies in terms of absolute value, however, there are still several sites showing fluxes with relatively high values in the range 150–340 g $m^{-2}$ $d^{-1}$. In consideration of the fact that both soil $CO_2$ fluxes and hypocenter depth globally increase when moving away from PdF, these relatively high flux values take on a greater significance.

The most substantial superimposition between earthquakes and the $CO_2$ flux anomalies is observed where the seismic events are deepest, more than 20 km. Figure 7c shows that the highest values of $CO_2$ flux are measured on the vertical of a narrow N30-40 seismic zone located at the border between PdN and PdF volcanic edifices. Particularly interesting is the high $CO_2$ flux recorded in the SW part of the zone, where a significant cluster of deep and unusually intense volcano tectonic events was recorded a few months after the large 2007 caldera-forming eruption [*Di Muro et al*., 2015].

To summarize, the cross correlation of $CO_2$ flux and earthquake distribution reveals a sharp decoupling for the shallow level (above 11 km bsl) while correlation increases with higher hypocenter depth. The best correlation is observed along the N30-40 zone. Less clear is the possible correlation between the anomalous degassing area close to the SE rift and the deep seismicity, where the maximum density of the deep earthquakes is recorded off the coastline. Finally, there is no specific evidence of correlations between $CO_2$ flux and seismicity along the NE rift. Nevertheless, inside the Enclos Fouqué caldera immediately south of the NE rift, a well-defined cluster of deep earthquakes with a general E-W orientation does show a rather good correlation with the anomalous $CO_2$ flux (Figure 7c). As discussed further, NE and SE rifts zones are important pathways of lateral magma transfer in recent times [*Michon et al*., 2013].

### 5.2. PdF Cone Density Distribution and $CO_2$ Flux

Cinder cones develop on eruptive fissures which open along the dyke path. Therefore, their distribution is considered as delineating preferential intrusion paths, which are also named as rift zones [*Walker*, 1999]. In our study, we used data from *Michon et al*. [2015] and *Morandi et al*. [2016]. Consequently, using a similar approach employed for the comparison of the seismic events and the $CO_2$ flux anomalies, we correlated the spatial distribution of the $CO_2$ flux and of the eruptive cones (Figure 8). Even if our survey was, to some degree, spatially limited by morphological obstacles and by the dense tropical vegetation resulting in a not entirely homogenous distribution of $CO_2$ flux measurements, most of the highest flux values are recorded in areas of high cone concentration. This correlation is especially visible for the NE, SE, and NW-SE rift zones. Regarding the NW-SE rift zones, as already shown above, this alignment overlays a deep seismic zone, while the summit zone lacks any $CO_2$ flux anomaly most probably because of the high density of fractures and/or deep fluid pressurization. Concerning the South Volcanic Zone, the very low $CO_2$ fluxes combined with the lack of any seismicity and absence of recent eruptions may indicate a current inactivity of this area. Therefore, at first glance, data suggest that the $CO_2$ flux anomalies are concentrated above areas of deep seismicity and/or along recently active volcanic zones (1977 and 1986 for the NE and SE rift zones, respectively; 15–17 century for the NW-SE rift zone). However, two points here are worth noting: (i) magmas emplaced along the NE and SE rift zones are similar to those involved in the Enclos Fouqué caldera, where fractionation and degassing processes in the shallow plumbing system has taken place (shallower than 11 km bsl) [*Albarède et al*., 1997; *Di Muro et al*., 2014, 2015; *Michon et al*., 2015]; (ii) activity along the NE and SE rift zones is relatively rare (three and five eruptions during the last 315 years along the NE and SE rift zones, respectively [*Michon et al*., 2013]) and, in general, the lowermost eruptive fissures have produced highly degassed lavas [*Delorme et al*., 1989; *Kieffer et al*., 1977]. However, we need to stress that detailed knowledge of the actual spatial distribution of the peripheral part of PdF magma storage system is still lacking.

### 5.3. PdF Volcano-Tectonic Structures and $CO_2$ Flux

The structural inheritance of the oceanic lithosphere is recognized as a parameter of primary importance in the control of the volcano-tectonic structures of intraplate volcanoes such as Hawaii [*MacDonald*, 1972],

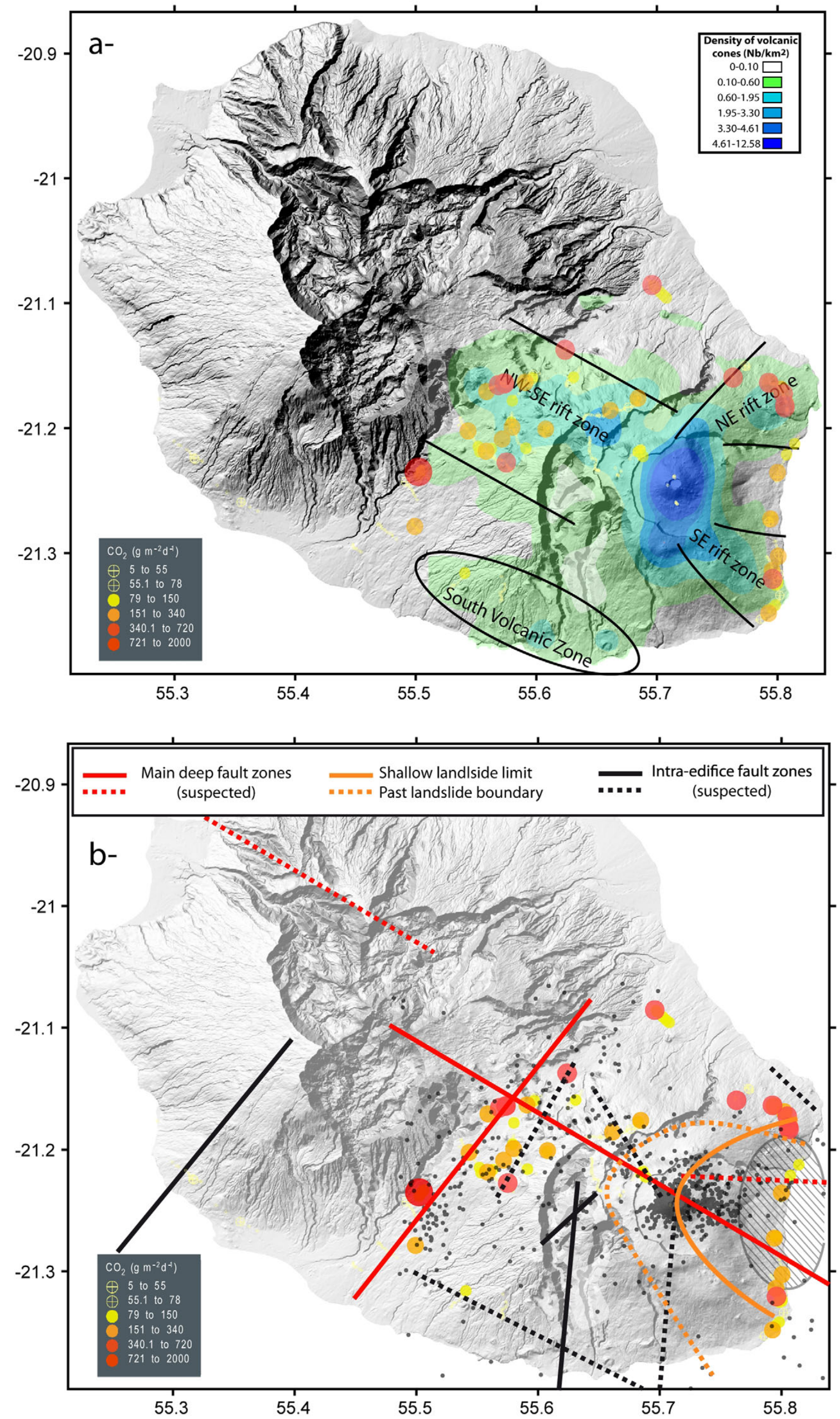


**Figure 8.** (a) Plot showing the spatial distribution of $CO_2$ fluxes and the superimposed map of eruptive cones and of the main structural features. (b) Synthesis of volcano-tectonic structures described for La Réunion. Deep (lithospheric) structures (red lines) are parallel to the main N30 and N120 directions of the oceanic lithosphere [*Michon et al.*, 2007] and control the deep magma transfer of Piton de la Fournaise [*Michon et al.*, 2015]. Intraedifice structures correspond to (1) fault or fault zones (black lines) that may control magma ascent to form volcanic zones [*Bonali et al.*, 2011; *Michon et al.*, 2007] or (2) the limits of past or active flank destabilizations. Also shown is the seismicity recorded by the OVPF/IPGP network and the intrusive complex identified by gravity anomaly (elliptic grey area filled by lines) [*Malengreau et al.*, 1999; *Gailler and Lénat*, 2010].

Canaries [*Carracedo*, 1994], or Azores [*Navarro et al.*, 2009]. In La Réunion, such a control has also been proposed to explain the parallel orientations of, on the one hand, the spreading ridges and transform faults of the oceanic crust and, on the other, the rift zones of Piton des Neiges and Piton de la Fournaise [*Bonali* *et al*., 2011; *Michon et al*., 2007]. Furthermore, a control of the inherited lithospheric structures has recently been put forward in relation to the geometry of the deep plumbing system and of the main rift zones of Piton de la Fournaise [*Michon et al*., 2015]. Here the deepest part of the plumbing system below 20 km bsl, which corresponds to the N30-40 deep seismic zone observed between the summits of Piton des Neiges and Piton de la Fournaise, is parallel to the oceanic transform faults (Figure 8b), while the NW-SE segment of the plumbing system between 11 and 20 km bsl, also made visible by the seismicity, would be controlled by shallower lithospheric structures. In such a structural framework, we propose that west of the PdF summit the exsolved $CO_2$ at depth follows the inherited structures of the lithosphere during its ascent (Figure 8b).

Questions remain on the origin of the high $CO_2$ flux along the NE and SE rift zones. Despite a lack of robust constraints, we propose the following interpretation combining secondary deep magma transfer zones and edifice heterogeneities to explain the location of the $CO_2$ anomalies on the NE and SE flanks of PdF. Seismic data reveal the occurrence of a deep (between 20 and 40 km bsl) N90 trending small seismic zone below the E flank of PdF (Figures 7c and 8b). This seismic cluster is parallel to the magnetic anomalies of the oceanic lithosphere locally found east of La Réunion, between the island and the Mauritius Transform Fault [*Lénat et al*., 2001]. Whether this zone corresponds to a magma transfer zone or not is uncertain, but similar deep seismic zones of deep magma transfer paths have been identified at Kilauea [*Klein et al*., 1987]. The $CO_2$ degassing related to the N90 magma transfer zone would be deviated by two structural means. Shallow (i.e., intraedifice) structures like the landslides scar of the Plaine des Sables or the active flank creep of the PdF East flank could channel $CO_2$ migration through the surface along their lateral rims. Moreover, the eastern flank of Piton de la Fournaise overlays a large intrusive complex, identified by a deep drill hole [*Rançon et al*., 1989], and a large gravity anomaly (Figure 8b) [*Gailler and Lénat*, 2010; *Malengreau et al*., 1999]. This large intrusive body, whose thickness was estimated at $\sim$4 km from gravity data [*Gailler and Lénat*, 2010; *Malengreau et al*., 1999], is made of a gabbro, dunite, and wherlite, which lack any porosity and show microfractures sealed by secondary minerals [*Lerebour et al*., 1989]. In addition, occurrence of recent events of magma transfer and temporary storage below the eastern flank has only recently been recognized [*Di Muro et al*., 2014].

On the basis of available data, we tentatively propose that $CO_2$ degassing occurs related to magma transfer and storage below the E flank of PdF and that its ascent inside the edifice is deviated by the large intrusive body, following its outer perimeter. Generally speaking, the significance of intermediate depth seismicity below the eastern flank and of deep seismicity at the southern boundary of the NE rift is still unclear and could suggest that deep levels of magma transfer and storage are shifted in relation to the volcano summit.

### 5.4. Summary Discussion

This study takes into consideration the combination of soil $CO_2$ flux measurements with the analysis of the isotopic signature and puts them in the general volcano-tectonic context of the Piton de la Fournaise massif. The correlation of the findings of our geochemical survey with the seismic events of the last 8 years, the distribution of the pyroclastic cones density and the orientation of the main volcano-tectonic structures, give us the opportunity to present the following remarks:

1. Our chemical and isotopic data set indicates that a significant (up to 50 wt %) portion of the soil $CO_2$ flux has a magmatic origin. This is most evident in sites with an anomalous flux against the background where isotopic composition results from a binary mixing between a deep magmatic end-member and a shallow biogenic source (Figures 4 and 5). This is the first recorded evidence of the occurrence of volcanic $CO_2$ emanations through the soil of large parts of PdF volcanic massif.
2. The spatial distribution of anomalous $CO_2$ emissions is clearly linked with the main and recently active rift zones cutting the PdF massif as identified by the distribution of recent volcano-tectonic events and of pyroclastic cones.
3. The low fluxes recorded in the central area show that the link between soil emissions and seismic and volcanic activity is complex. This has already been shown in studies of other active and inactive volcanoes, such as in Italy, Hawaii, Azores, and Canary [*Giammanco et al*., 1998, 2006; *Hernández et al*., 1998, 2000; *Viveiros et al*., 2010], where it has been well documented that the volcanic degassing path of soil $CO_2$ flux is closely linked with the distribution of the main structural lineaments. However, further

measurements are required to test whether $CO_2$ flux actually increases during phases of higher volcanic activity in the case of PdF

4. Deep (mantle lithosphere; >20 km) seismic events match very well with the distribution of $CO_2$ soil emissions at the surface of PdF. This is consistent with current geochemical models demonstrating the low solubility of $CO_2$ in basaltic magmas and the consequent early separation from the melt at high pressure and great depth [*Holloway and Blank*, 1994; *Lesne et al*., 2011; *Papale et al*., 2006]. Melt and fluid inclusion studies at PdF permit the tracking of $CO_2$ exsolution in a broad range of depths (up to 7 kbar) (see *Di Muro et al*., [2016], for a review). Interestingly, melt and fluid inclusions record higher magma storage pressures below the NW-SE rift zone, where deep seismic events occur, than in the Enclos Fouqué caldera, where seismicity is shallower. Shallower pressures (typically <1 kbar) and hypocenters are a typical feature of the central area of PdF area. Consequently, low $CO_2$ fluxes in the central area could also stem from the multistep ascent and storage of small volumes of degassed magmas at shallow depth below the central area [*Di Muro et al*., 2015] together with deep gas pressurization [*Savage et al*., 2015]. More than 50% of initial $CO_2$ content is exsolved from the basaltic magma at a pressure lower than 400 MPa, approximately corresponding to a depth lower than 15 km. This means that the deep magmatic source of PdF begins to degas a significant fraction of its primary $CO_2$ content at higher depth, thus generating the anomalous $CO_2$ fluxes best detected in the distal portions of the volcano.
5. The survey took place during a quiescent period of PdF, that is, during a time with very low background seismicity and in a phase of general deflation of the volcano. This factor can further explain the low rate of $CO_2$ emissions detected near the central area. Therefore, our survey represents the basis for the definition of background levels of $CO_2$ soil degassing and for the ongoing program of installation of permanent geochemical stations, which could potentially detect significant changes of $CO_2$ flux levels during future phases of volcanic activity.
6. The conceptual models that have been constructed for the PdF shallow plumbing system converge in the recognition that no large magma body exists at shallow level below the PdF central cone [e.g., *Albarède et al*., 1997; *Di Muro et al*., 2014, 2015; *Massin et al*., 2011; *Prono et al*., 2009]. Magma is possibly stored in a set of small volume sills with variable degrees of connection. The low degree of degassing of the PdF central area is in agreement with the absence of important volumes of magma at shallow level. Recent petrologic and geochemical analyses suggest that post-2007 activity involved distinct pockets of shallow degassed magma with little inputs of deeper melts [*Di Muro et al*., 2015]. Consequently, the volcanic contribution detected in the soil of the volcanic massif is mostly likely related to degassing of deep magmas, periodically feeding the shallow part of the plumbing system.

## 6. Conclusion

Our geochemical survey has identified areas of anomalous soil $CO_2$ flux whose isotopic composition records a significant (up to 50 wt %) magmatic signature. The distribution of $CO_2$ flux anomalies is correlated with that of seismic and volcanic activity on the three main rift (NE, SE, and NW-SE) zones cutting the massif of Piton de la Fournaise and of major lithospheric discontinuities (N30-40) located at the boundary between Piton des Neiges and Piton de la Fournaise volcanoes.

The strongest anomalies occur in proximity of sites of recent and deep (>20 km; at mantle lithosphere depth) seismicity. Low emissions are recorded close to the central area, consistently with (a) the phase of quiescence of the volcano during the surveys, (b) the absence of large volumes of magma stored below the volcano central cone, and (c) the high density of fractures in the summit area. Our data suggest that the crossing of the main regional tectonic lineaments on the rift zones controls the distribution of the anomalous gas fluxes and point to a clear link with the deep plumbing system of the Piton de la Fournaise volcano.

Regular and systematic monitoring of $CO_2$ degassing on this very active volcano in the areas identified by the study would therefore not only provide invaluable information of potential precursors to new inputs of magma but may also facilitate the prediction of imminent eruptive activity and consequently play a significant role in the planning of civil defense strategies in conditions of high risk such as eccentric eruptions.

**Acknowledgments**
We thank INSU (CNRS) and La Réunion Préfecture (Projet pour la quantification de l'aléa volcanique à La Réunion) for funding part of the survey activities performed in this study. We are very grateful to Fausto Grassa (INGV-Palermo) for his useful suggestions and the isotope analysis. Special thanks to G. P. A Torres (IGN—Spain) for supplying the software for the *Sinclair* [1974] procedure. We are also particularly grateful to the reviewers, T. Fischer, and F. Viveiros for their useful comments that have substantially contributed to the improvement of this paper. All the new data in this paper are included as four tables in an supporting information file; any additional data may be obtained from Marco Liuzzo (e-mail: marco.liuzzo@ingv.it). Seismic data are available for academic purposes through the Datacenter IPGP (http://centrededonnees.ipgp.fr/); structural and cone density data are available from the authors upon request (dimuro@ipgp.fr). The source code (beta version) for the Sinclair procedure used in this study is available from the author upon request (Pedro Torres, Instituto Geográfico Nacional, Spain, patorres@fomento.es).

## References

Albarède, F., B. Luais, G. Fitton, M. Semet, E. Kaminski, B. G. J. Upton, P. Bachèlery, and J. L. Cheminée (1997), The geochemical regimes of Piton de la Fournaise volcano (Réunion) during the last 530,000 years, *J. Petrol.*, *38*, 171–201.

Allard, P., et al. (1991), Eruptive and diffuse emissions of $CO_2$ from Mt. Etna, *Nature*, *351*, 387–390.

Amundson, R., L. Stern, T. Baisden, and Y. Wang (1998), The isotopic composition of soil and soil-respired $CO_2$, *Geoderma*, *82*, 83–114.

Baret, S., M. Rouget, D. M. Richardson, C. Lavergne, B. Egoh, J. Dupont, and D. Strasberg (2006), Current distribution and potential extent of the most invasive alien plant species on La Réunion (Indian Ocean, Mascarene Islands), *Aust. Ecol.*, *31*, 747–758.

Barillon, R., S. Violette, E. Nicolini, D. Klein, A. Chambaudet, J. P. Carbonnel, M. J. Heath, and J. Merefield (1993), Continuous measurements of radon content in groundwater on the volcanic site of Piton de la Fournaise (Island of Réunion, France), *Nucl. Tracks Radiat. Meas.*, *22*, 277–280.

Basile-Doelsch, I., R. Amundson, W. E. E. Stone, C. A. Masiello, J. Y. Bottero, F. Colin, F. Masin, D. Borschneck, and J. D. Meunier (2005), Mineralogical control of organic carbon dynamics in a volcanic ash soil on La Réunion, *Eur. J. Soil Sci., 56, 689–703*, doi:10.1111/j.1365-2389.2005.00703.x.

Basile-Doelsch, I., R. Amundson, W. E. E. Stone, D. Borschneck, J. Y. Bottero, S. Moustier, F. Masin, and F. Colin (2007), Mineral control of carbon pools in a volcanic soil horizon, *Geoderma*, *137*, 477–489, doi:10.1016/j.geoderma.2006.10.006.

Bonali, F. L., C. Corazzato, and A. Tibaldi (2011), Identifying rift zones on volcanoes: An example from La Réunion island, Indian Ocean, *Bull. Volcanol.*, *73*, 347–366, doi:10.1007/s00445-010-0416-1.

Bonforte, A., C. Federico, S. Giammanco, F. Guglielmino, M. Liuzzo, and M. Neri (2013), Soil gases and SAR measurements reveal hidden faults on the sliding flank of Mt. Etna (Italy), *J. Volcanol. Geotherm. Res.*, *251*, 27–40.

Bosch, D., J. Blichert-Toft, F. Moynier, B. K. Nelson, P. Telouk, P. Y. Gillot, and F. Albarède (2008), Pb, Hf and Nd isotope compositions of the two Réunion volcanoes (Indian Ocean): A tale of two small-scale mantle blobs, *Earth Planet. Sci. Lett.*, *265*, 748–768.

Camarda, M., S. Gurrieri, and M. Valenza (2006a), $CO_2$ flux measurements in volcanic areas using the dynamic concentration method: Influence of soil permeability, *J. Geophys. Res.*, *111*, B05202, doi:10.1029/2005JB003898.

Camarda, M., S. Gurrieri, and M. Valenza (2006b), In situ permeability measurements based on a radial gas advection model: Relationships between soil permeability and diffuse $CO_2$ degassing in volcanic areas, *Pure Appl. Geophys.*, *163*(4), 897–914, doi:10.1007/s00024-006-0045-y.

Carracedo, J. C. (1994), The Canary Islands: An example of structural control on the growth of large oceanic-island volcanoes, *J. Volcanol. Geotherm. Res.*, *60*, 225–241.

Cerling, T. E., D. K. Solomon, J. Quade, and J. R. Bowman (1991), On the isotopic composition of carbon in soil carbon dioxide, *Geochim. Cosmochim. Acta*, *55*, 3403–3405.

Chiodini, G., R. Avino, T. Brombach, S. Caliro, C. Cardellini, S. De Vita, F. Frondini, E. Marotta, and G. Ventura (2004), Fumarolic degassing west of Mount Epomeo, Ischia (Italy), *J. Volcanol. Geotherm. Res.*, *133*, 291–309.

Chiodini, G., S. Caliro, C. Cardellini, R. Avino, D. Granieri, and A. Schmidt (2008), Carbon isotopic composition of soil $CO_2$ efflux, a powerful method to discriminate different sources feeding soil $CO_2$ degassing in volcanic-hydrothermal areas, *Earth Planet. Sci. Lett.*, *274*(3–4), 372–379, doi:10.1016/j.epsl.2008.07.051.

Courtillot, V., J. Besse, D. Vandamme, R. Montigny, J.-J. Jaeger, and H. Cappetta (1986), Deccan flood basalts at the Cretaceous-Tertiary boundary?, *Earth Planet Sci. Lett.*, *80*, 361–374.

Delorme, H., P. Bachèlery, P. A. Blum, J. L. Cheminée, J. F. Delarue, C. J.-C. Delmond, A. Hirn, J. C. Lepine, P. Vincent, and J. Zlotnicki (1989), March 1986 eruptive episodes at Piton de la Fournaise volcano (Reunion island), *J. Volcanol. Geotherm. Res.*, *36*, 199–208.

Di Muro, A., A. Aiuppa, M. Burton, N. Metrich, P. Allard, T. Fougeroux, G. Giudice, and R. Guida (2012), *Intra-Eruptive Gas Emissions and Shallow Magma Storage After the 2007 Summit Caldera Collapse of Piton de la Fournaise, Reunion Island*, EGU, Vienna.

Di Muro, A., N. Métrich, D. Vergani, M. Rosi, P. Armienti, T. Fougeroux, E. Deloule, I. Arienzo, and L. Civetta (2014), The shallow plumbing system of Piton de la Fournaise Volcano (La Réunion Island, Indian Ocean) revealed by the major 2007 caldera forming eruption, *J. Petrol.*, *55*, 1287–1315, doi:10.1093/petrology/egu025.

Di Muro, A., T. Staudacher, V. Ferrazzini, N. Métrich, P. Besson, C. Garofalo, and B. Villemant (2015), Shallow magma storage at Piton de la Fournaise volcano after 2007 summit caldera collapse tracked in Pele's hairs, in *Hawaiian Volcanoes: From Source to Surface, AGU Monogr. Ser*., edited by R. J. Carey et al., chap. 9, pp. 189–212, AGU, Washington, D. C., doi:10.1002/9781118872079.ch9.

Di Muro, A., N. Métrich, P. Allard, A. Aiuppa, M. Burton, B. Galle, and T. Staudacher (2016), Magma degassing at Piton de la Fournaise volcano, in *Active Volcanoes of the Southwest Indian Ocean, Active Volcanoes World Ser*., edited by P. Bachèlery et al., pp. 203–222, Springer, Berlin.

Doelsch, E., V. Van de Kerchove, and H. Saint Macary (2006), Heavy metal content in soils of Réunion (Indian ocean), *Geoderma*, *134*, 119–134.

Duncan, R. A., J. Backman, and L. Peterson (1989) Reunion hotspot activity through tertiary time: Initial results from the ocean drilling program, leg 115, *J. Volcanol. Geotherm. Res.*, *36*, 193–198.

Frank, A. B., M. A. Liebig, and J. D. Hanson (2002), Soil carbon dioxide fluxes in northern semiarid grasslands, *Soil Biol. Biochem.*, *34*, 1235–1241.

Frank, A. B., M. A. Liebig, and D. L. Tanaka (2006), Management effects on soil $CO_2$ efflux in northern semiarid grassland and cropland, *Soil Tillage Res.*, *89*, 78–85, doi:10.1016/j.still.2005.06.009.

Gailler, L. S., and J. F. Lénat (2010), Three-dimensional structure of the submarine flanks of La Réunion inferred from geophysical data, *J. Geophys. Res.*, *115*, B12105, doi:10.1029/2009JB007193.

Gailler, L.-S., J. F. Lénat, M. Lambert, G. Levieux, N. Villeneuve, and J.-L. Froger (2009), Gravity structure of Piton de la Fournaise volcano and inferred mass transfer during the 2007 crisis, *J. Volcanol. Geotherm. Res.*, *184*, 199–207, doi:10.1016/j.jvolgeores.2009.01.024.

Giammanco, S., S. Gurrieri, and M. Valenza (1998), Anomalous soil $CO_2$ degassing in relation to faults and eruptive fissures on Mount Etna (Sicily, Italy), *Bull. Volcanol.*, *60*, 252–259, doi:10.1007/s004450050231.

Giammanco, S., S. Gurrieri, and M. Valenza (2006), Fault controlled soil $CO_2$ degassing and shallow magma bodies: Summit and lower East Rift of Kilauea Volcano (Hawaii), 1997, *Pure Appl. Geophys.*, *163*(4), 853–867, doi:10.1007/s00024-006-0039-9.

Gurrieri, S., and M. Valenza (1988), Gas transport in natural porous mediums: A method for measuring $CO_2$ flows from the ground in volcanic and geothermal areas, *Rend. Soc. Ital. Mineral. Petrol.*, *43*, 1151–1158.

Gurrieri, S., M. Liuzzo, and G. Giudice (2008), Continuous monitoring of soil $CO_2$ flux on Mt. Etna: The 2004–2005 eruption and the role of regional tectonics and volcano tectonics, *J. Geophys. Res.*, *113*, B09206, doi:10.1029/2007JB005003.

Hanyu, T., T. J. Dunai, G. R. Davies, I. Kaneoka, S. Nohda, and K. Uto, (2001), Noble gas study of the Reunion hotspot: Evidence for distinct less-degassed mantle sources, *Earth Planet. Sci. Lett.*, *193*, 83–98.

Hernández, P., N. M. Pérez, J. M. Salazar, S. Nakai, K. Notsu, and H. Wakita (1998), Diffuse emission of carbon dioxide, methane, and helium-3 from Teide Volcano, Tenerife, Canary Islands, *Geophys. Res. Lett.*, *25*, 3311–3314, doi:10.1029/98GL02561.

Hernández, P., N. Pérez, J. M. Salazar, M. Sato, K. Notsu, and H. Wakita (2000), Soil gas $CO_2$, $CH_4$, and $H_2$ distribution in and around Las Cañadas caldera, Tenerife, Canary Islands, Spain, *J. Volcanol. Geotherm. Res.*, *103*, 425–438, doi:10.1016/S0377-0273(00)00235-3.

Holloway, J. R., and J. G. Blank (1994), Application of experimental results to C–O–H species in natural melts, in *Volatiles in Magmas, Reviews in Mineralogy*, edited by M. R. Carroll and J. R. Holloway, pp. 185–230, Mineral. Soc. of Am., Washington, D. C.

Hopp, J., and M. Trieloff (2005), Refining the noble gas record of the Reunion mantle plume source: Implications on mantle geochemistry, *Earth Planet. Sci. Lett.*, *240*(3–4), 573–588, doi:10.1016/j.epsl.2005.09.036.

Ilyinskaya, E., et al. (2015), Degassing regime of Hekla volcano 2012–2013, *Geochim. Cosmochim. Acta*, *159*, 80–99, doi:10.1016/j.gca.2015.01.013.

Irwin, W. P., and I. Barnes (1980), Tectonic relations of carbon dioxide discharges and earthquakes, *J. Geophys. Res.*, *85*, 3115–3121, doi:10.1029/JB085iB06p03115.

Kieffer, G., B. Tricot, and P. M. Vincent (1977), Une éruption inhabituelle (Avril 1977) du Piton de la Fournaise (Ile de la Réunion): Ses enseignements volcanologiques et structuraux, *C. R. Acad. Sci. Paris*, *285*, 957–960.

Klein, F. W., R. Y. Koyanagi, J. S. Nakata, and W. R. Tanigawa (1987), The seismicity of Kilauea's magma system, in *Volcanism in Hawaii*, edited by R. W. Decker et al., *U.S. Geol. Surv. Prof. Pap., 1350(2)*, 1019–1185.

Lénat, J., B. Gibert-Malengreau, and A. Galdeano (2001), A new model for the evolution of the volcanic island of Reunion (Indian Ocean), *J. Geophys. Res.*, *106*, 8645–8663.

Lerebour, P., J. P. Rançon, and T. Augé (1989), The Grand Brûlé exploration drilling: New data on the deep frame-work of the Piton de la Fournaise volcano. Part II: Secondary minerals, *J. Volcanol. Geotherm. Res.*, *36*, 129–137.

Lesne, P., S. C. Kohn, J. Blundy, F. Witham, R. E. Botcharnikov, and H. Behrens (2011), Experimental simulation of closed-system degassing in the system basalt-$H_2O$-$CO_2$-S-Cl, *J. Petrol.*, *52*, 1737–1762, doi:10.1093/petrology/egr027.

Liuzzo, M., S. Gurrieri, G. Giudice, and G. Giuffrida (2013), Ten years of soil $CO_2$ continuous monitoring on Mt. Etna: Exploring the relationship between processes of soil degassing and volcanic activity, *Geochem. Geophys. Geosyst.*, *14*, 2886–2899, doi:10.1002/ggge.20196.

Liuzzo, M., G. Giudice, A. Di Muro, V. Ferrazzini, and L. Michon (2014), New observational evidence of $CO_2$ degassing anomalies on the Piton de la Fournaise and the relationship between seismotectonic structures and $CO_2$ flux from the soil, in *Geophysical Research Abstracts*, vol. 16, EGU Gen. Assem., Vienna.

MacDonald, G. A. (1972), *Volcanoes*, 510 pp., Prentice Hall, Englewood Cliffs, N. J.

Malengreau, B., J. F. Lénat, and J.-L. Froger (1999), Malengreau-Reunion Island (Indian Ocean) inferred from the interpretation of gravity anomalies, *J. Volcanol. Geotherm. Res.*, *88*, 131–146.

Marty, B., V. Meynier, E. Nicolini, E. Griesshaber, and J. P. Toutain (1993), Geochemistry of gas emanations: A case study of the Réunion hot spot, Indian ocean, *Appl. Geochem.*, *8*, 141–152.

Massin, F., V. Ferrazzini, P. Bachèlery, A. Nercessian, Z. Duputel, and T. Staudacher (2011), Structures and evolution of the plumbing system of Piton de la Fournaise volcano inferred from clustering of 2007 eruptive cycle seismicity, *J. Volcanol. Geotherm. Res.*, *202*, 96–106.

Michon, L., F. Saint-Ange, P. Bachèlery, N. Villeneuve, and T. Staudacher (2007), Role of the structural inheritance of the oceanic lithosphere in the magmato-tectonic evolution of Piton de la Fournaise volcano (La Réunion Island), *J. Geophys. Res.*, *112*, B04205, doi:10.1029/2006JB004598.

Michon, L., A. Di Muro, N. Villeneuve, P. Fadda, F. Manta, and C. Saint-Marc (2013), Explosive activity of the summit cone of Piton de la Fournaise volcano: A historical and geological review, *J. Volcanol. Geotherm. Res.*, *263*, 117–133, doi:10.1016/j.jvolgeores.2013.06.012.

Michon, L., V. Ferrazzini, A. Di Muro, N. Villeneuve, and V. Famin (2015), Rift zones and magma plumbing system of Piton de la Fournaise volcano: How do they differ from Hawaii and Etna, *J. Volcanol. Geotherm. Res.*, *303*, 112–129.

Mielnick, P. C., and W. A. Dugas (2000), Soil $CO_2$ flux in a tallgrass prairie, *Soil Biol. Biochem.*, *32*, 221–228.

Moldrup, P., S. Yoshikawa, T. Olesen, T. Komatsu, and D. E. Rolston (2003), Gas diffusivity in undisturbed volcanic ash soils: Test of soil-water-characteristic based prediction models, *Soil Sci. Soc. Am. J.*, *67*, 41–51.

Morandi, A., C. Principe, A. Di Muro, G. Leroi, L. Michon, and P. Bachèlery (2016), Pre-historic explosive activity at Piton de la Fournaise volcano, in *Active Volcanoes of the Southwest Indian Ocean, Active Volcanoes World Ser.*, edited by P. Bachèlery et al., pp. 107–138, Springer, Berlin.

Navarro, A., N. Lourenço, J. Chorowicz, J. M. Miranda, and J. Catalão (2009), Analysis of geometry of volcanoes and faults in Terceira Island (Azores): Evidence for reactivation tectonics at the EUR/AFR plate boundary in the Azores triple junction, *Tectonophysics*, *465*, 98–113, doi:10.1016/j.tecto.2008.10.020.

Papale P., R. Moretti, and D. Barbato (2006), The compositional dependence of the saturation surface of $H_2O + CO_2$ fluids in silicate melts, *Chem. Geol.*, *229*, 78–95.

Peltier, A., T. Staudacher, and P. Bachèlery (2010), New behaviour of the Piton de La Fournaise volcano feeding system (La Réunion Island) deduced from GPS data: Influence of the 2007 Dolomieu caldera collapse, *J. Volcanol. Geotherm. Res.*, *192*, 48–56, doi:10.1016/j.jvolgeores.2010.02.007.

Pietruszka, A. J., E. H. Hauri, and J. Blichert-Toft (2009), Crustal contamination of mantle-derived magmas within Piton de la Fournaise, Réunion Island, *J. Petrol.*, *50*, 661–684.

Prono, E., J. Battaglie, V. Monteiller, J. L. Got, and V. Ferrazzini (2009), P-wave velocity structure of Piton de la Fournaise volcano deduced from seismic data recorded between 1996–1999, *J. Volcanol. Geotherm. Res.*, *184*, 49–62.

Rançon, J. P., P. Lerebour, and T. Augé (1989), The Grand Brûlé exploration drilling: New data on the deep framework of the Piton de la Fournaise volcano. Part 1: Lithostratigraphic units and volcanostructural implications, *J. Volcanol. Geotherm. Res.*, *36*, 113–127.

Rey, A., E. Pegoraro, V. Tedeschi, I. De Parri, P. G. Jarvis, and R. Valentini (2002), Annual variation in soil respiration and its components in a coppice oak forest in Central Italy, *Global Change Biol.*, *8*, 851–866, doi:10.1046/j.1365-2486.2002.00521.x.

Rouff, A. A., B. L. Phillips, S. G. Cochiara, and K. L. Nagy, (2012), The Effect of dissolved humic acids on aluminosilicate formation and associated carbon sequestration, *Appl. Environ. Soil Sci.*, *2012*, 12, doi:10.1155/2012/430354.

Roult, G., A. Peltier, T. Staudacher, V. Ferrazzini, B. Taisne, A. Di Muro, and the OVPF team (2012), A comprehensive classification of the Piton de la Fournaise eruptions (La Réunion Island) spanning the 1986–2010 period. Search for eruption precursors from the broad-band GEOSCOPE RER station analysis and interpretation in terms of volcanic processes, *J. Volcanol. Geotherm. Res.*, *241*, 78–104.

Savage, M. K., et al. (2015), Seismic anisotropy and its precursory change before eruptions at Piton de la Fournaise volcano, La Reunion, *J. Geophys. Res. Solid Earth*, *120*, 3430–3458, doi:10.1002/2014JB011665.

Seidel, J. L., A. Bonneville, and J. F. Lenat (1988), Radon measurements related to Piton de la Fournaise (Réunion) from 1983 to 1987, *C. R. Acad. Sci. Paris*, *306*, 89–92.

Sinclair, A. J. (1974), Selection of threshold values in geochemical data using probability graphs, *J. Geochem. Explor.*, *3*, 129–149.
Staudacher, T., V. Ferrazzini, A. Peltier, P. Kowalski, P. Boissier, P. Catherine, F. Lauret, and F. Massin (2009), The April 2007 eruption and the Dolomieu crater collapse, two major events at Piton de la Fournaise (La Réunion Island, Indian Ocean), *J. Volcanol. Geotherm. Res.*, *184*(1–2), 126–137, doi:10.1016/j.jvolgeores.2008.11.005.
Strasberg, D., M. Rouget, D. M. Richardson, S. Baret, J. Dupont, and R. M. Cowling (2005), An assessment of habitat diversity and transformation on La Réunion Island (Mascarene Islands, Indian Ocean) as a basis for identifying broad-scale conservation priorities, *Biodiversity Conserv.*, *14*, 3015–3032.
Toutain, J. P., J. C. Baubron, and L. François (2002), Runoff control of soil degassing at an active volcano. The case of Piton de la Fournaise, Réunion Island, *Earth Planet. Sci. Lett.*, *19*, 83–94.
Trieloff, M., J. Kunz, and C. J. Allégre (2002), Noble gas systematics of the Réunion mantle plume source and the origin of primordial noble gases in Earth's mantle, *Earth Planet. Sci. Lett.*, *200*, 297–313.
Viveiros, F., T. Ferreira, J. Cabral Vieira, C. Silva, and J. L. Gaspar (2008), Environmental influences on soil $CO_2$ degassing at Furnas and Fogo volcanoes (São Miguel Island, Azores archipelago), *J. Volcanol. Geotherm. Res.*, *177*(4), 883–893, doi:10.1016/j.jvolgeores.2008.07.005.
Viveiros, F., C. Cardellini, T. Ferreira, S. Caliro, G. Chiodini, and C. Silva (2010), Soil $CO_2$ emissions at Furnas volcano, São Miguel Island, Azores archipelago: Volcano monitoring perspectives, geomorphologic studies, and land use planning application, *J. Geophys. Res.*, *115*, B12208, doi:10.1029/2010JB007555.
Viveiros, F., J. Vandemeulebrouck, A. P. Rinaldi, T. Ferreira, C. Silva, and J. V. Cruz (2014), Periodic behavior of soil $CO_2$ emissions in diffuse degassing areas of the Azores archipelago: Application to seismovolcanic monitoring, *J. Geophys. Res. Solid Earth*, *119*, 7578–7597, doi:10.1002/2014JB011118.
Vlastélic, I., C. Deniel, C. Bosq, P. Télouk, P. Boivin, P. Bachèlery, V. Famin, and T. Staudacher (2009), Pb isotope geochemistry of Piton de la Fournaise historical lavas, *J. Volcanol. Geotherm. Res.*, *184*(1–2), 63–78, doi:10.1016/j.jvolgeores.2008.08.008.
Walker, G. P. L. (1999), Volcanic rift zones and their intrusion swarms, *J. Volcanol. Geotherm. Res.*, *94*, 21–34, doi:10.1016/S0377-0273(99)00096-7.